

Dynamic Quantification of the Atom Rearrangement Behavior with Al-Mg 5052 Undercooling Liquid Film

Eisaku Tokuchi and Kimioku Asai*

Department of Mechanical Engineering, Musashi Institute of Technology, Tamazutumi, Setagaya-ku, Tokyo 158-8557

(Received October 22, 2002)

The atom rearrangement behaviors along with the rapid solidification and high temperature oxidation of an interdendritic liquid (liquid film) with an arc spot-fused A5052 sheet were experimentally investigated in comprehensive terms of the solidification progress, concentration, and temperature by using high-speed breaking and breakage techniques. The latter is a new quenching method with an aqueous solution of surface-active agents to prevent the fractured section from the selective diffusion of Mg coupled with high temperature oxidation. Continuous liquid films of the fractured-section (solidification) layers were analyzed by XPS as well as fractography with FE-SEM. In a surfactant experiment, the results verified that the characteristic diffusion during oxidation occurred with the driving force being electrostatic attraction. Concerning the solidification behavior of rapidly solidifying columnar dendrite, the results of XPS measurements indicated that after a tip undercooling of about 25 °C the liquid solute concentration increased exponentially with decreasing temperature, while taking a solute concentration path below the T0 curve (in binary system analysis). The fractography was in qualitative agreement with the solute concentration result in terms of the mass balance by showing restricted lateral solidification progress.

A number of attempts have been made to quantify the atom rearrangement behavior during crystal growth. In the area of casting or ingot solidification,[1–8] solid-state diffusion had been theoretically considered with Fick's law, which succeeded in describing the large solute concentrations in the liquid and the resulting segregation. Recent studies on atom rearrangement in this area of liquid–solid transformation have been focusing on rapid solidification or multicomponent behavior with state-of-the-art computer simulations,[9] which have been addressing the problem of the interface solute partitioning phenomenon in solidification reaction. The atomic scale behavior is also of great interest in the area of nano or oxidation-related technology, such as semiconductors.[10]

The experimental methods established here with arc spot-fusion sheets involve measurements of the temperature with thermocouples,[11,12] the liquid distributions in the solid-liquid coexisting zone with a high-speed breaking technique and fractography,[11,13] and the atom rearrangement behaviors in two reactions, i.e., solidification accompanied by solute partitioning phenomenon and high temperature oxidation coupled with the characteristic diffusion process,[14] with fractured sections liquid films, XPS (X-ray Photoelectron Spectroscopy) solute concentration measurements, and a new quenching breakage technique to improve the XPS measurement accuracy in terms of the influence of the selective high temperature oxidation of fractured sections. Continuous liquid films on the fractured sections form in the interaction with the outside gas, while the original solid-liquid interface proceeds after the rapid fracture formation. Therefore, the conservation of the original solute concentration in the liquid is the most important factor in considering the measurement accuracy to quantify the solute partitioning behavior with by a surface analysis such as XPS or AES (Auger Electron Spectroscopy). In this case, solute diffusion in the film thickness direction must be averted.

On the other hand, the diffusion in the area of the oxidation reaction is generally explained by the electrostatic attraction of the ion effect between oxygen and metal. That is, it is realized that if the diffusion coupled with oxidation is driven by an electrostatic attraction of an ion effect, it means that intentionally applying static charge becomes a feasible reaction control. Therefore, the present experimental method, which is able to investigate the behaviors at the metal liquid–gas interface, provides two benefits.

Experimental

The material used was Al-alloy A5052-H3, whose compositions are given in Table 1. Sheets of 1 mm thickness were sheared into a rectangular shape of 140 × 80 mm. Ar-gas tungsten arc spot-fusion on a welding torch was performed at the center of the specimen with an arc current (direct-current electrode positive) of 40 A, an arc voltage of 20 V, an arc length (distance from the specimen to the electrode tip) of 3 mm, an arc time of 10 s, and a shielding Ar-gas flow rate of 10 L/min and a time of 15 s. Under this fusion condition, the fusion-portion became a two-dimensional bead, and the diameter of 9.8 mm was assured with an accuracy of ±0.3 mm. The solidification progressed from the fusion boundary through the center of the fusion spot counter-radiately to the heat conduction flux, forming a cellular dendrite with a dendrite arm spacing of about 7 μm. A temperature measurement[11,12] was performed with a chromel/alumel (Type k) thermocouple having a wire diameter of 150 μm. Immediately after the arc current was automatically cut off, as shown in Fig. 1, a high-speed breaking machine rapidly loaded and ruptured the specimen at a given time from the arc stop in the longitudinal direction with a breaking speed of about 750 mm/s;[11,13] the solidifying fusion-portion became semicircular with almost the same thickness as that of the

Table 1. Chemical Compositions of A5052 (wt%).

Mg	Fe	Si	Cu	Cr	Mn	Zn	Al
2.62	0.19	0.09	0.04	0.22	0.03	0.02	bal.

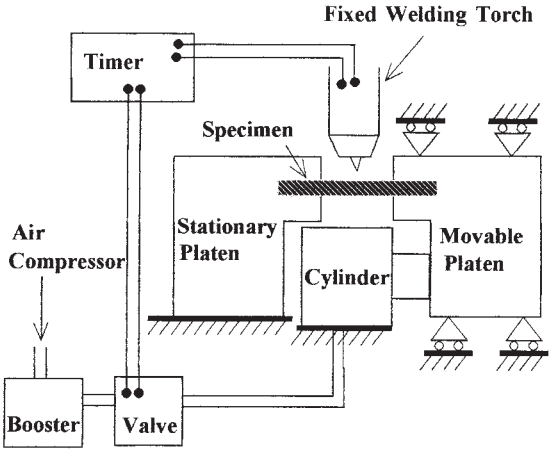

Fig. 1. Schematic principle of high-speed-breaking experiment.

specimen with respect to the solid-liquid coexisting zone. Fractography followed the breaking operation. FE-SEM (Field Emission Scanning Electron Microscopy) was used with an acceleration voltage of 1 kV. In this observation, the distribution of the liquid films in each fractured section was carefully quantified as a function of the time elapsed from the arc stop and the distance from the fusion boundary.[11,13] Small-Spot XPS (X-ray Photoelectron Spectroscopy) was employed to quantify the fractured sections solute concentrations. The minimum diameter of the X-ray spot was 150 μm. Ar-ion sputtering was also performed for concentration depth profiles in the liquid film. The etching rate was 1 Å/s in SiO_2, approximated as 0.3 Å/s in Al_2O_3, and 1–2 Å/s in pure Al.

In an attempt to prevent the high temperature oxidation of the fractured sections, the present study adopted a new quenching method involving an anti-oxidation effect of surface-active agents. The surface-active agents was a detergent containing sodium alkyl sulfate, sodium α-alkene sulfonate, fatty acid diethanol amide, lauric acid diethanol amide, and alkylamine oxide. As shown in Fig. 2, the arc-spot-fused specimen was kept horizontally using a jig apparatus; after completion of the fusion process, the solidifying specimen was quickly put into the aqueous surfactant solution; this protected the fractured section of a self-contraction running crack from oxidation. The specimen for an XPS measurement was ultrasonically cleaned in pure water, followed by methanol, and then analyzed.

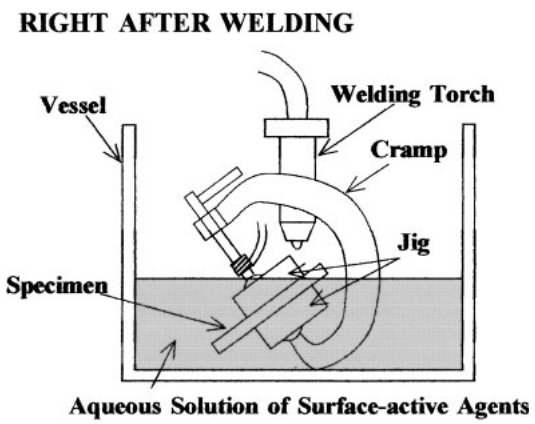

Fig. 2. Schematic principle of a quenching method with an aqueous solution of surface-active agents to prevent the fractured sections from the Mg selective diffusion in high temperature oxidation.

Results

Microscopic Detail of Fractured Sections. Figure 3 shows a magnified view of a fractured section near the solidification front that underwent a displacement of the interdendritic liquid with the impact of high-speed breaking. It must be realized that shrinkage grooves formed along the grain boundaries. In addition, the thickness of the liquid was measurable by using a discernible interdendritic cavity left after the interdendritic liquid was blown away. Because the undercooling from the solidification front temperature (625 °C) was about 10 °C to 25 °C (34 °C to 49 °C in total undercooling from the melting point of 649 °C), a low fraction-solid fracture is beyond doubt. Theoretically, the lateral thickening of the cellular dendrite dominantly depends on the solute pile-up at the tip.[15] Therefore, the above experimental facts mean that the solute pile-up at the tip was quite small.

High Temperature Oxidation of Liquid Films. Figure 4 is Continuous Cooling Solidification Process (CCSP) diagram,[11–13] containing the results of XPS measurements for oxidized, non-sputtered fractured sections in high-speed breaking. In the diagram, (Ⅰ) defined by the thick curves represents complete liquid in the fusion zone (: weld metal: W.M.), (Ⅱ) the continuous liquid film stage in W.M., (Ⅲ) the solid cohesion stage in W.M., (Ⅳ) complete solid in W.M., (Ⅴ) the continuous liquid film stage in the partial fusion zone (: HAZ), (Ⅵ) the solid cohesion stage in HAZ, and (Ⅶ) complete solid in HAZ. The first thick-curve dividing (Ⅰ) and (Ⅱ) corresponds to the locus of the solidification front. The results of temperature measurements are also shown by the isotherms. The axial dendrite growth and temperature gradient are shown by the vertical relations. The undercoolings at the solidification front, at the onset of the solid cohesion stage, and at the complete solidification end, are shown by the three thick curves in the upper side of the diagram, respectively. At a given position, the thickness (volume) of an interdendritic liquid (liquid film) continuously decreases as the time elapses; thereby, the appearance of the fracture surface continuously alters, accordingly, from continuous liquid film through a film-dimple transition to a compete dimple.

The results of XPS measurements at the outer surface showed excessive Mg concentrations compared with the binary eutectic of 35 wt%, reaching 89 wt% at maximum. The Mg concentrations

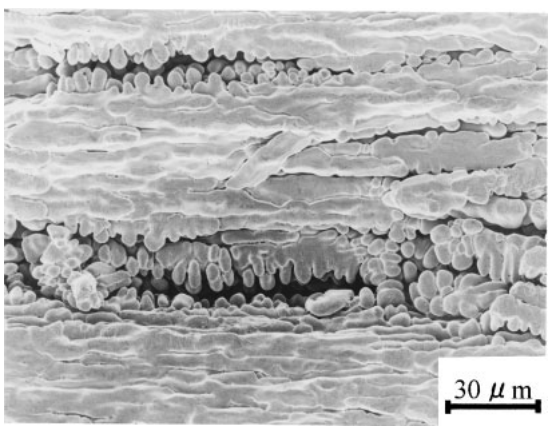

Fig. 3. Photomicrograph of a fractured section near the solidification front in a high-speed breaking sample; the solidification front is situated in right side of the photo.

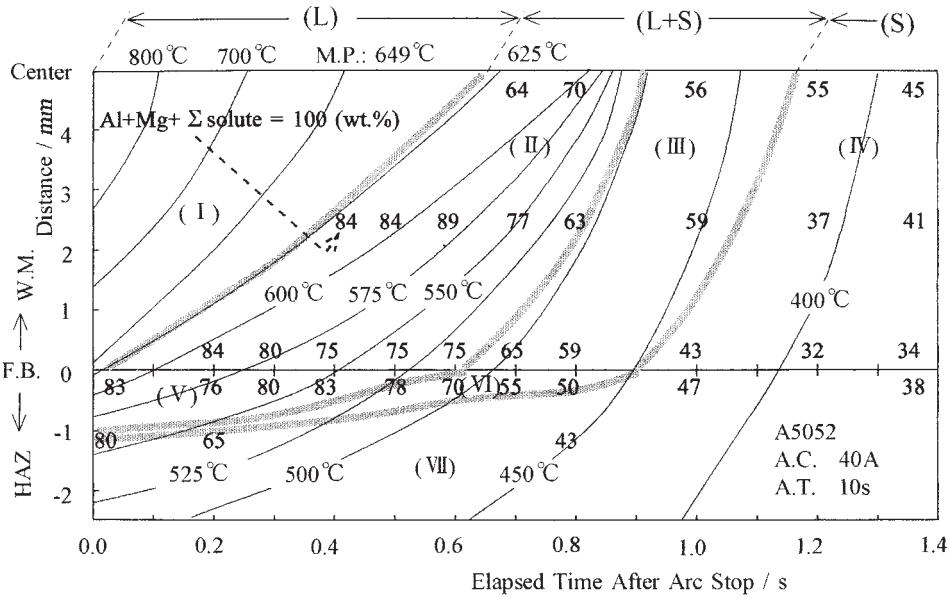

Fig. 4. Continuous Cooling Solidification Process (CCSP) diagram showing the solute concentrations at the non-sputtered liquid film surfaces in high temperature oxidized fractured sections of high-speed-breaking-XPS experiment; showing the results of temperature measurement and fractography by the isotherms and the thick curves, respectively.

decreased with temperature decrease.

Figure 5 shows the depth profiles of the surface liquid film. The data is from a sample with a 0.5 s breaking time and 2.2 mm from the fusion boundary. There is a negative concentration gradient of Mg, and the Mg concentration inside the liquid film reaches about 3 wt%. Throughout the measurements, the spectrum of Mg did not shift as pure Mg, but as Mg oxide. In addition, pure Al was detected in 0 s of sputtering as well as Al oxide, and after 200 s of sputtering the Al oxide peak disappeared. From these results, it was found that the surface oxidation film was completely removed by Ar-ion sputtering.

Quenching Experiment using an Aqueous Surfactant Solution. A quenching experiment with an aqueous surfactant solution is capable of coping concurrently with the problems on high temperature oxidation and conservation of the original solute concentration. Figure 6 shows the statistics of XPS measurements in three different cases with pure water, cylinder oil, and the presently adopted aqueous solution of surface-active agents. The result shows that the anti-oxidation effect of surface-active agents is the most useful, preventive measure in the Mg selective oxidation.

Figure 7 shows two depth-profile results for a medium-fraction solid in a surfactant experiment. Both of the Mg distributions are almost uniform over the film thickness direction. The results also indicate entirely higher Mg concentrations than those in Fig. 5 of the high-speed-breaking experiment, despite the same position in the fractured section. This is because of a time lapse in the fracture of quenching. With regard to the other elements contained in the used material, Si and Fe were detected; rarely was there a small percent of Cu. In Fig. 7, □ and ○ indicate the values for the case that the sputtered portion was oxidized for tens of seconds at room temperature again, which are a reference to indicate the actual concentrations inside the liquid film. For the main spectrum peak of Si in XPS overlaps a peak of Al when the influence of surface

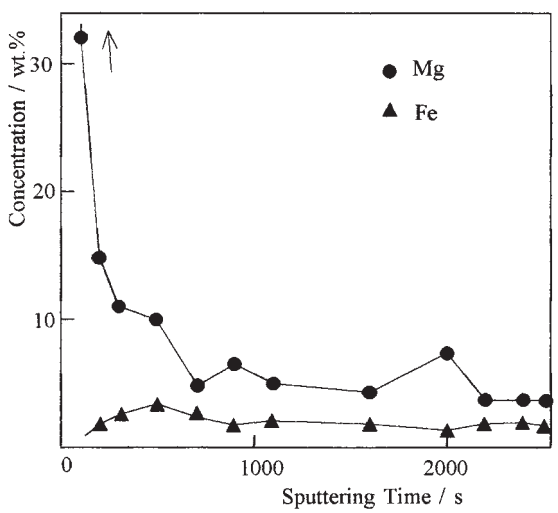

Fig. 5. XPS depth profiles in a fractured section of low-fraction solid obtained with high-speed breaking.

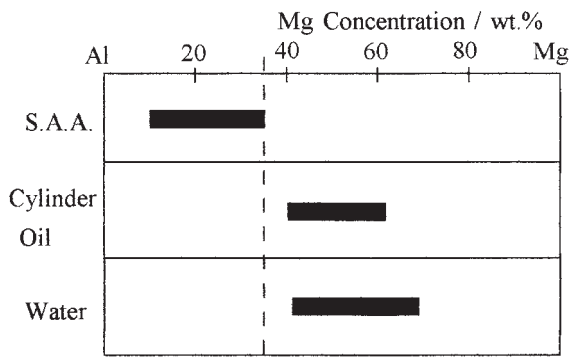

Fig. 6. Statistics of XPS measurements in quenching, non-sputtered experiment with three different cases of an aqueous solution of surface-active agents (S.A.A.), pure water, and cylinder oil.

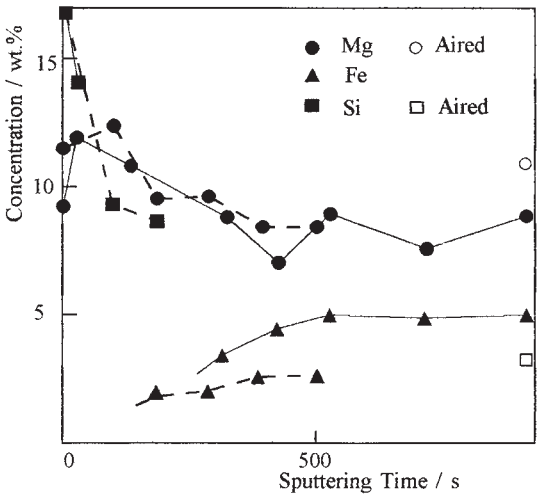

Fig. 7. XPS depth profiles for two different samples of surface-active-agent experiment in medium fraction solid.

oxides and contaminations on computation becomes small.

Discussion

Verification of Electrically Driven Diffusion in an Oxidation Reaction. Because the atom jump in the absence of an electrostatic field occurs with the same probability for different directions, the reaction atom is unable to concentrate heterogeneously. Hence, the other possible factors that are against the electrically driven diffusion of oxidation are solidification segregation of the liquid film and the effect of the gas–bulk interface. Regarding the latter factor, even if Mg atoms concentrate at the metal liquid–gas interface, after being oxidized, they can no longer selectively diffuse towards the metal liquid–oxide interface under the condition of no electrostatic field.

In Fig. 6, a comparison between pure water and SAA denies the former factor and verifies the atom rearrangement in which an oxidation reaction occurs with an electrically driven diffusion of the ion effect. As a reason for the substantial reduction in the Mg concentration in the SAA experiment, the cooling-rate effect of quenching on the diffusion time would be impossible because the vaporization heat in the aqueous surfactant solution containing a small percent of detergent must be remarkably larger than that of water. Hence, the possible factors are limited to the effect of the surface-active agents contained in the aqueous solution. The first is a decrease in the oxygen partial pressure, where oxygen molecules were physically absent. Otherwise, The second is that oxygen atoms or molecules were ionized by the surfactant and, thereby, Al oxidation predominantly occurred. In the first factor, solidification segregation is denied as the reason for the Mg selective diffusion in the oxidized samples. In the second, if the Al atoms to be oxidized are not ionized before the diffusion process, solidification segregation is denied, and if ionized, the diffusion process is an electric one.

Reliability of the XPS Experiment. It can be found out from Figs. 4, 5, and 7 that the solute concentration path estimated for the actual solidification process is below the T0 curve of Al–Mg binary system. It is obvious that the solid–liquid interface does not behave as an equilibrium. In comprehensively considering all of the obtained results, the actual liquid concentration is supposed to increase exponentially with decreasing temperature. There are two possible reasons for this solute concentration behavior. The first is because of the restricted lateral solidification progress that was evidenced by the present fractography, although the connection between the restricted solidification progress and the interface nonequilibrium is thermodynamically unclear. Hence, the second is the effect of a partitionless interface movement due to the large undercooling from the liquidus. In either case, the reliability of the present XPS experiment is assured. Therefore, the question concerning interface thermodynamics related to the atom rearrangement mechanism of solidification progress is addressed in order to account for the relation between the suppressed solute concentration path and the progress restriction.

Conclusion

The purpose of the present experiments with the fractured sections liquid films of A5052 solidification was to investigate both dynamically and quantitatively the atom rearrangement behavior during rapid solidification and high temperature oxidation in terms of the solidification progress, temperature, and liquid solute concentration. The obtained conclusions are as follows:

(1) The quenching method with an aqueous surfactant solution was able to accurately quantify the liquid solute concentrations of solidification in the XPS measurement by preventing the fractured sections from the Mg selective oxidation.

(2) The atom rearrangement during the oxidation reaction is attributed to the electrically driven diffusion of the ion effect.

(3) The lateral thickening of rapid cellular solidification was restricted despite the fact of a large tip undercooling of about 25 °C. The results of XPS measurements were in qualitative agreement with the restricted solidification progress by quantitatively showing a suppressed solute concentration path below the T0 curve in binary system analysis. These facts address the question of interface thermodynamics.

(4) The measurement data presented in this report is applicable to broad interests of atomic scale because of the above conclusion (2).

The authors gratefully acknowledge Professor Emeritus Shozaburo Ohta, Professor Shinichi Ohya, Technical Engineer Takefumi Higase, Dr. Akira Yoshida, and Technical Engineer Emi Shindo, in our research institute, and all others for their advice and support.

References

1 G. H. Gulliver, *J. Inst. Metals.*, **1913**, 120.
2 E. Scheil, *Z. Metallkd.*, **34**, 70 (1942).
3 W. G. Pfann, *Trans. TMS-AIME.*, **194**, 747 (1952).
4 H. D. Brody and M. C. Flemings, *Trans. TMS-AIME.*, **236**, 615 (1966).
5 T. W. Clyne and W. Kurz, *Metall. Mater. Trans. A.*, **12**, 965 (1981).
6 T. Matsumiya, H. Kajioka, S. Mizoguchi, Y. Ueshima, and H. Esaka, *Trans. ISIJ.*, **24**, 873 (1984).
7 I. Ohnaka, *Trans. ISIJ.*, **24**, 1045 (1986).
8 S. Kobayashi, *Trans. ISIJ.*, **28**, 728 (1988).
9 A. Nogami and T. Matumiya, *J. JWS.*, **66**, 6 (1997).
10 T. Ito, "Computer-jyou no kessyouseityou," Kyouritu-syuppan, Tokyo (2002).

11 K. Asai, Dr. Thesis, Musashi Institute of Technology (1993).
12 S. Ohta, K. Asai, and S. Ohya, *Trans. JWS.*, **16**, 35 (1985).
13 S. Ohta and K. Asai, *Trans. JWS.*, **24**, 140 (1993).
14 O. Kubaschewski and B. E. Hopkins, ''Oxidation of Metals and Alloys,'' Butterworths Publications, London (1953), pp. 130–137.
15 B. Giovanola and W. Kurz, *Metall. Mater. Trans. A.*, **21**, (1990).